ЖЭТФ, 2014, том 145, вып. 4, стр. 671–676

ON THE EINSTEIN–CARTAN COSMOLOGY VS. PLANCK DATA

*D. Palle**

Zavod za teorijsku fiziku, Institut Rugjer Bošković
Bijenička cesta 54, 10000 Zagreb, Croatia

Received November 11, 2013

The first comprehensive analyses of Planck data reveal that the cosmological model with dark energy and cold dark matter can satisfactorily explain the essential physical features of the expanding Universe. However, the inability to simultaneously fit the large and small scale TT power spectrum, the scalar power index smaller than unity, and the observations of the violation of the isotropy found by few statistical indicators of the CMB urge theorists to search for explanations. We show that the model of the Einstein–Cartan cosmology with clustered dark matter halos and their corresponding clustered angular momenta coupled to torsion can account for small-scale–large-scale discrepancy and larger peculiar velocities (bulk flows) for galaxy clusters. The nonvanishing total angular momentum (torsion) of the Universe enters as a negative effective density term in the Einstein–Cartan equations causing partial cancellation of the mass density. The integrated Sachs–Wolfe contribution of the Einstein–Cartan model is negative, and it can therefore provide partial cancellation of the large-scale power of the TT CMB spectrum. The observed violation of the isotropy appears as a natural ingredient of the Einstein–Cartan model caused by the spin densities of light Majorana neutrinos in the early stage of the evolution of the Universe and bound to the lepton CP violation and matter–antimatter asymmetry.

DOI: 10.7868/S0044451014040090

1. INTRODUCTION AND MOTIVATION

Although the presence of dark matter and dark energy is justified by all cosmological observations, their identification and properties are still far from being established. The measurements of the CMB fluctuations are in this respect especially valuable because of the wealth and accurate information that can be extracted from them.

The most recent disclosed results of the Planck mission contain issues like the temperature power spectrum, gravitational lensing or the integrated Sachs–Wolfe (ISW) effect, up to the Sunyaev–Zeldovich cluster counts, and isotropy, and non-Gaussianity of the cosmic infrared background. It seems that the old, unexpected features, beyond the ΛCDM + inflation model persist in data and are even more highlighted: 1. the large-scale temperature power spectrum much lower than the ΛCDM prediction, limited not only to the low quadrupole [1] but also to almost all multipole moments $l < 30$ (see Fig. 37 in Ref. [2]), 2. the scalar power spectrum index less than 1 (see Table 8 in Ref. [2]), 3. violation of isotropy observed as hemispherical asymmetry, parity asymmetry, quadrupole–octopole alignment, cold spots, and dipolar asymmetry [3].

If the violation of isotropy will be confirmed by other complementary cosmic observations of radio galaxies [4], spiral galaxies [5], bulk flows of clusters [6], or quasars [7], it will challenge cosmological principles and call for new theoretical insights.

Assuming that the observed anomalies are real phenomena, we try to understand and elucidate the measured physical features by the Einstein–Cartan (EC) cosmology. Incorporating rotating degrees of freedom of matter (spin and angular momentum) and space-time (torsion) into the relativistic framework, the EC cosmology appears as a nonsingular theory [8, 9]; the cosmic mass density can be fixed [9], the scalar power index can acquire a negative tilt [10], and spin densities trigger density fluctuations [11] and the right-handed vorticity (rotation) of the Universe [12] resulting at later stages of the evolution in the nonvanishing total angular momentum of the Universe [13]. The nonsingular EC cosmology is in conformity with the nonsingular theory of gauge interactions in particle physics [14] that contains light and heavy Majorana neutrinos as hot and cold dark matter particles [15], including other important implications of the perturbative and nonper-

*E-mail: palle@irb.hr

turbative aspects of strong and electroweak interactions phenomenology [16].

In this paper, we investigate and compare EC and ΛCDM cosmologies solving evolution equations for the scale-dependent density contrasts, mass fluctuations, peculiar velocities, and the integrated Sachs–Wolfe effect. In the next section, we describe the evolution equations and definitions and introducte our simple clustering model. The concluding section deals with the numerical results of the computations, comparisons of the EC and ΛCDM cosmologies, and final remarks and hints for future research.

2. DEFINITIONS, EQUATIONS, AND THE CLUSTERING MODEL

Because any deviation from cosmic homogeneity and isotropy is very small, we limit our considerations to the homogeneous and isotropic geometry. We start the evolution in the radiation era when the clustering of dark and baryonic matter is negligible. The evolution equations for matter density contrasts in Fourier space are derived in [17]:

$$\begin{aligned} &\frac{d^2h}{dt^2} + \frac{2}{a}\frac{da}{dt}\frac{dh}{dt} = 8\pi G_N(2\rho_r\delta_r + \rho_m\delta_m), \\ &\frac{d\delta_m}{dt} = \frac{1}{2}\frac{dh}{dt}, \quad \frac{d\delta_r}{dt} = \frac{4}{3}\left(\frac{kv}{a} + \frac{1}{2}\frac{dh}{dt}\right), \\ &\frac{dv}{dt} = -k\frac{\delta_r}{4a}, \\ &\left(\frac{da}{dt}\right)^2 = \frac{8}{3}\pi G_N a^2(\rho_r + \rho_m + \rho_\Lambda). \end{aligned} \qquad (1)$$

We here use the notation

$$h = \sum_{\alpha=1}^{3} h_\alpha^\alpha, \quad g_{\alpha\beta} = -a^2[\delta_{\alpha\beta} - h_{\alpha\beta}],$$

density contrasts are

$$\delta_i = \frac{\delta\rho_i}{\rho_i},$$

k is the comoving wave number,

$$a = \frac{R}{R_0} = \frac{1}{1+z},$$

subscripts m, r, and Λ denote matter, radiation and the cosmological constant quantities, and v is a velocity. All the quantites are functions of t and $\vec{k}$.

These equations can be cast into a more suitable form by eliminating

$$h = \sum_{\alpha=1}^{3} h_\alpha^\alpha$$

and by changing the evolution variable to $y = \ln a$:

$$\begin{aligned} \frac{d^2\delta_m}{dy^2} &= -\frac{1}{2}\frac{d\delta_m}{dy}\Omega_m(\Omega_r a^{-1} + \Omega_m + \Omega_\Lambda a^3)^{-1} + \\ &+ \frac{3}{2}(2\Omega_r\delta_r + \Omega_m a\delta_m)(\Omega_r + \Omega_m a + \Omega_\Lambda a^4)^{-1}, \\ \frac{d\delta_r}{dy} &= \frac{4}{3}\left(\frac{d\delta_m}{dy} + \frac{kv}{\dot{a}}\right), \quad \frac{dv}{dy} = -\frac{\delta_r}{4}\frac{k}{\dot{a}}. \end{aligned} \qquad (2)$$

Our notation includes

$$\rho_r = \Omega_r\rho_c a^{-4}, \quad \rho_m = \Omega_m\rho_c a^{-3},$$

$$\rho_\Lambda = \Omega_\Lambda\rho_c, \quad \rho_c = \frac{3H_0^2}{8\pi G_N},$$

$$H_0 = 100h \text{ km}\cdot\text{s}^{-1}\cdot\text{Mpc}^{-1}$$

and

$$\dot{a} = 3.2409\cdot 10^{-18}h\left[\Omega_r a^{-2} + \Omega_m a^{-1} + \Omega_\Lambda a^2\right]^{1/2}\text{s}^{-1}.$$

The evolution equations for the EC cosmology, neglecting small vorticity and acceleration

$$\omega = m = 0, \quad \lambda = 0, \quad Q = Q_0 a^{-3/2} = \text{torsion},$$

are derived in [13] (Eq. (14)):

$$\begin{aligned} &\ddot{\delta}_1 + 2\frac{\dot{a}}{a}\dot{\delta}_1 - 2Q\dot{\delta}_2 + \left(-\frac{1}{3}\kappa\Lambda - \frac{5}{3}Q^2 - \right. \\ &\qquad \left. - \frac{1}{3}\kappa\rho + \frac{\ddot{a}}{a}\right)\delta_1 + \frac{1}{4}\frac{\dot{a}}{a}Q\delta_2 = 0, \\ &\ddot{\delta}_2 + 2\frac{\dot{a}}{a}\dot{\delta}_2 + 2Q\dot{\delta}_1 + \left(-\frac{1}{3}\kappa\Lambda - \frac{5}{3}Q^2 - \right. \\ &\qquad \left. - \frac{1}{3}\kappa\rho + \frac{\ddot{a}}{a}\right)\delta_2 - \frac{1}{4}\frac{\dot{a}}{a}Q\delta_1 = 0, \\ &\ddot{\delta}_3 + 2\frac{\dot{a}}{a}\dot{\delta}_3 + \left(-\frac{1}{3}\kappa\Lambda - \frac{2}{3}Q^2 - \frac{1}{3}\kappa\rho + \frac{\ddot{a}}{a}\right)\delta_3 = 0, \\ &\delta \equiv [\delta_1^2 + \delta_2^2 + \delta_3^2]^{1/2}. \end{aligned} \qquad (3)$$

We assume that after the redshift $z_G = 10$, the nonlinear bound structures are formed in the form of stars, galaxies, and clusters. The clustering of particles forming halos is described by a model with only two parameters k_G and σ_G. This is applied to both mass and angular momentum clustering:

$$\begin{aligned} Q(a) &= (2\pi)^{-3}\int d^3k\hat{Q}(a,\vec{k}) = \\ &= Q_0 a^{-3/2}\Theta(z_G - z), \\ \hat{Q}(a,\vec{k}) &= \bar{Q}_0 a^{-3/2}\exp(-|k-k_G|/\sigma_G)\times \\ &\times\Theta(z_G - z) \Rightarrow Q_0 = \bar{Q}_0(2\pi)^{-3}\times \\ &\times\int d^3k\exp(-|k-k_G|/\sigma_G), \end{aligned} \qquad (4)$$

$$\rho(a) = (2\pi)^{-3}\int d^3k\hat{\rho}(a,\vec{k}) = \rho_0 a^{-3}\Theta(z_G - z),$$
$$\hat{\rho}(a,\vec{k}) = \bar{\rho}_0 a^{-3}\exp(-|k-k_G|/\sigma_G)\Theta(z_G - z) \Rightarrow \quad (5)$$
$$\Rightarrow \rho_0 = \bar{\rho}_0(2\pi)^{-3}\int d^3k\exp(-|k-k_G|/\sigma_G).$$

Fourier transformations of evolution equations (3) take the following form:

$$\left(\frac{\dot a}{a}\right)^2\frac{d^2\Delta_{1,2}}{dy^2} + \frac{\dot a}{a}\left(\frac{d\dot a}{da}+\frac{\dot a}{a}\right)\frac{d\Delta_{1,2}}{dy} \mp \mp 2\frac{\dot a}{a}\langle Q\frac{d\delta_{2,1}}{dy}\rangle_{FT} + \left(-\frac{1}{3}\kappa\Lambda + \frac{\ddot a}{a}\right)\Delta_{1,2} - -\frac{1}{3}\kappa\langle\rho_m\delta_{1,2}\rangle_{FT} - \frac{5}{3}\langle Q^2\delta_{1,2}\rangle_{FT} \pm \pm\frac{1}{4}\frac{\dot a}{a}\langle Q\delta_{2,1}\rangle_{FT} = 0, \quad (6)$$
$$\left(\frac{\dot a}{a}\right)^2\frac{d^2\Delta_3}{dy^2} + \frac{\dot a}{a}\left(\frac{d\dot a}{da}+\frac{\dot a}{a}\right)\frac{d\Delta_3}{dy} + + \left(-\frac{1}{3}\kappa\Lambda + \frac{\ddot a}{a}\right)\Delta_3 - \frac{1}{3}\kappa\langle\rho_m\delta_3\rangle_{FT} - -\frac{2}{3}\langle Q^2\delta_3\rangle_{FT} = 0.$$

The Einstein–Cartan field equations define the cosmic clocks (see Eq. (15) in Ref. [13]) as follows:

$$\dot a = H_0\left[\Omega_m a^{-1} + \Omega_\Lambda a^2 - \frac{1}{3}a^2Q^2\right]^{1/2},$$
$$\frac{d\dot a}{da} = H_0\frac{1}{2}\left[\Omega_m a^{-1} + \Omega_\Lambda a^2 - \frac{1}{3}a^2Q^2\right]^{-1/2} \times \times\left[-\Omega_m a^{-2} + 2\Omega_\Lambda a + \frac{1}{3}aQ^2\right], \quad (7)$$
$$\frac{\ddot a}{a} = \frac{1}{3}\kappa\Lambda - \frac{1}{6}\kappa\rho + \frac{2}{3}Q^2.$$

The following definitions and convolutions are used in Eq. (6):

$$\Delta_i(y,\vec{k}) \equiv \int d^3x\exp(i\vec{k}\cdot\vec{x})\delta_i(y,\vec{x}),$$
$$\langle Q\delta_i\rangle_{FT}(y,\vec{k}) \equiv \int d^3x\exp(i\vec{k}\cdot\vec{x})Q(y,\vec{x})\delta_i(y,\vec{x}) = = (2\pi)^{-3}\int d^3k' Q(y,\vec{k}-\vec{k}')\Delta_i(y,\vec{k}'),$$
$$\langle Q^2\delta_i\rangle_{FT}(y,\vec{k}) \equiv \int d^3x\exp(i\vec{k}\cdot\vec{x})Q^2(y,\vec{x})\delta_i(y,\vec{x}) = = (2\pi)^{-6}\int d^3k'd^3k''\Delta_i(y,\vec{k}')Q(y,\vec{k}'') \times \times Q(y,\vec{k}-\vec{k}'-\vec{k}'').$$

Having all the evolution equations for the EC and ΛCDM cosmologies, we define initial conditions in the radiation era and choose the parameters of the models:

$$a_i = 10^{-8}, \quad \delta_r(a_i) = k^{1/2}a_i^2,$$
$$\delta_m(a_i) = \frac{3}{4}k^{1/2}a_i^2,$$
$$\frac{d\delta_r}{dy}(a_i) = 2k^{1/2}a_i^2,$$
$$\frac{d\delta_m}{dy}(a_i) = \frac{3}{2}k^{1/2}a_i^2, \quad v(a_i) = 0,$$

ΛCDM:

$$\Omega_m = 0.34, \quad \Omega_\Lambda = 0.66, \quad h = 0.67, \quad Q = 0,$$

EC:

$$\Omega_m = 2, \quad \Omega_\Lambda = 0, \quad h = 0.67,$$
$$Q = \begin{cases} 0, & z > 10, \\ -2.3a^{-3/2}, & 1 < z \le 10, \\ -\sqrt{3}a^{-3/2}, & 0 \le z \le 1. \end{cases}$$

Our choice of the torsion (angular momentum) parameters is guided by the condition that at the zero redshift, $\Omega_Q \approx -1$ [9, 13] (at the redshifts $1 \ge z \ge 0$, the galaxy clusters emerge, changing the total angular momentum contribution of the era $z > 1$), while at the earlier epoch $10 > z > 1$, our choice is guided by the condition to roughly match the correct cosmic clocks and the age of the Universe:

$$\tau_U(\mathrm{Gyr}) = \frac{10}{h}\int_{10^{-3}}^{1}\frac{da}{a}\left[\Omega_\Lambda + \Omega_m a^{-3} - \frac{1}{3}Q^2\right]^{-1/2},$$

$$\tau_U(\Lambda\mathrm{CDM}) = 13.89\ \mathrm{Gyr}, \quad \tau_U(\mathrm{EC}) = 13.29\ \mathrm{Gyr},$$
$$k_{min} = 10^{-3}\ \mathrm{Mpc}^{-1}, \quad k_{max} = 10^2\ \mathrm{Mpc}^{-1},$$
$$k_G = 1\ \mathrm{Mpc}^{-1}, \quad \sigma_G = 0.25\ \mathrm{Mpc}^{-1}.$$

We integrate the above evolution equations to the relative accuracy $\mathcal{O}(10^{-4})$ by lowering the integration steps until the required accuracy is reached. Equations (2) are solved for the evolution from $a_i = 10^{-8}$ to $a_G = 1/(1+z_G)$ and Eqs. (6) are then solved from $a_G = 1/(1+z_G)$ to $a = 1$. The Adams–Bashforth–Moulton predictor–corrector method is used for differential equation integrations (code of L. F. Shampine and M. K. Gordon, Sandia Laboratories, Albuquerque, New Mexico) and CUBA Library for Multidimensional Integrations [18]. The next section is devoted to the detailed exposure of the numerical results and comparison between the EC and ΛCDM models. The relevance of the results for the Planck data are also given here.

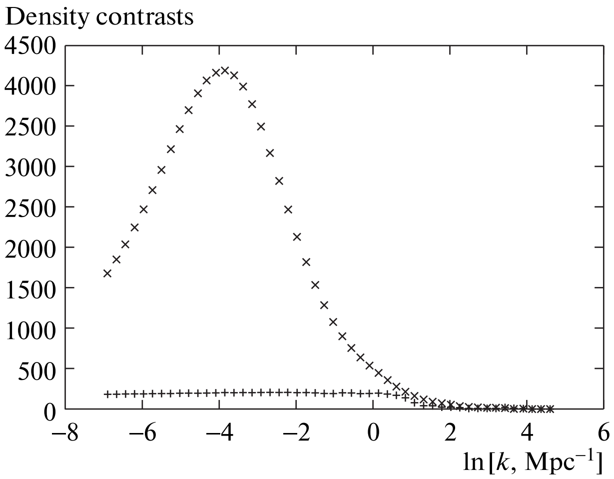

Fig. 1. Density contrasts at $z = 0$ as functions of the wave number k normalized at k_{max}: $\delta_m(k_{max}) = 1$. EC — $+$, ΛCDM — $\times$

3. RESULTS, DISCUSSION, AND CONCLUSIONS

Because the best fit to the Planck temperature power spectrum is dominantly performed by the multipoles $l > 30$, it is not surprising that the concordance ΛCDM model is favored, but at the expense of the wrong fit for low mutipoles (large scales). By solving evolution equations for the EC and ΛCDM with the simple clustering model, it can be verified that at low redshifts, these two models produce density contrasts that differ substantially at large scales, while being similar at smaller scales (see Fig. 1).

If we accept the following normalization on a larger scale [13]:

$$(\delta M/M)_{RMS}(a = 1, S_0 = 10\ \mathrm{h}^{-1} \cdot \mathrm{Mpc}) = 1,$$

then the processed spectra of mass fluctuations with the top hat window function for the EC and ΛCDM models differ at small scales (see Fig. 2):

$$\begin{aligned} &(\delta M/M)^2_{RMS}(a, S) \equiv \\ &\qquad \equiv N^{-1} \int d^3k W^2(\vec{k}, S)|\delta(a, \vec{k})|^2, \\ &N = \int d^3k W^2(\vec{k}, S_0)|\delta(a = 1, \vec{k})|^2, \\ &W(y = kS) = \frac{3}{y^3}(\sin y - y \cos y). \end{aligned} \tag{8}$$

We can similarly evaluate the peculiar velocities as functions of the scale and redshift with the same normalization as in Eq. (8):

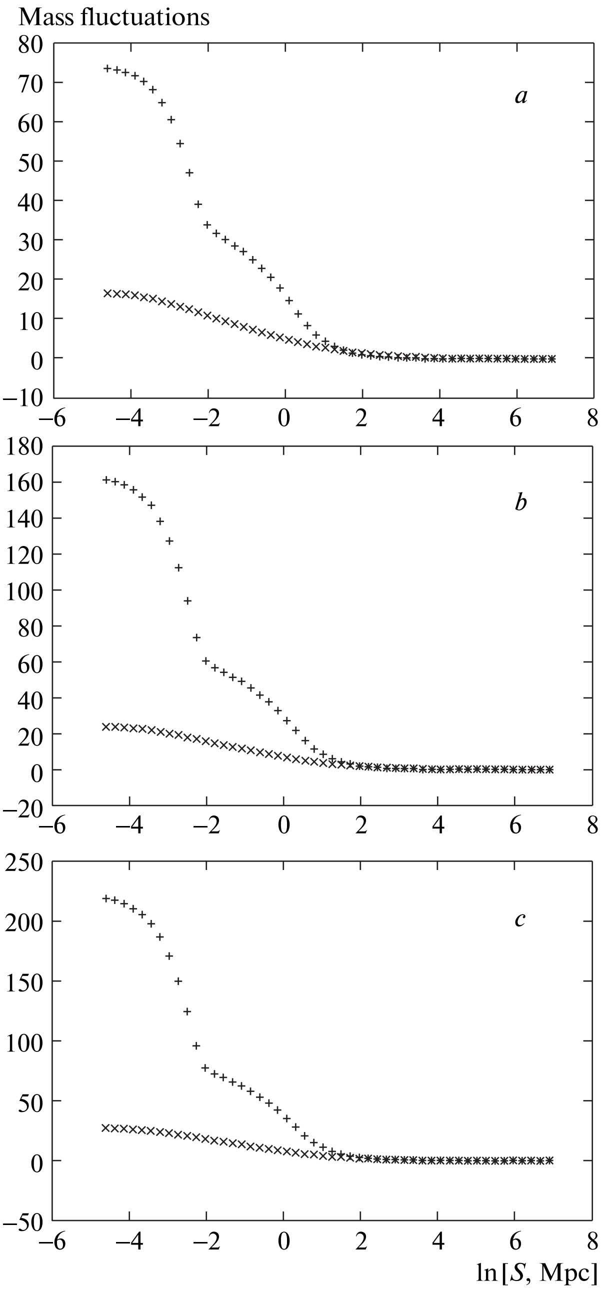

Fig. 2. Mass fluctuations for three redshifts ($z = 1$ (a), 0.25 (b), and 0 (c)) as functions of the scale S. EC — $+$, ΛCDM — $\times$

$$v^2_{RMS}(a, S) \equiv N^{-1} \int d^3k W^2(\vec{k}, S) \times \times \frac{1}{\vec{k}^2} \left| a\dot{a} \frac{d\delta(a, \vec{k})}{da} \right|^2, \tag{9}$$

giving the expected results (see Fig. 3), where the EC cosmology produces larger peculiar velocities than the

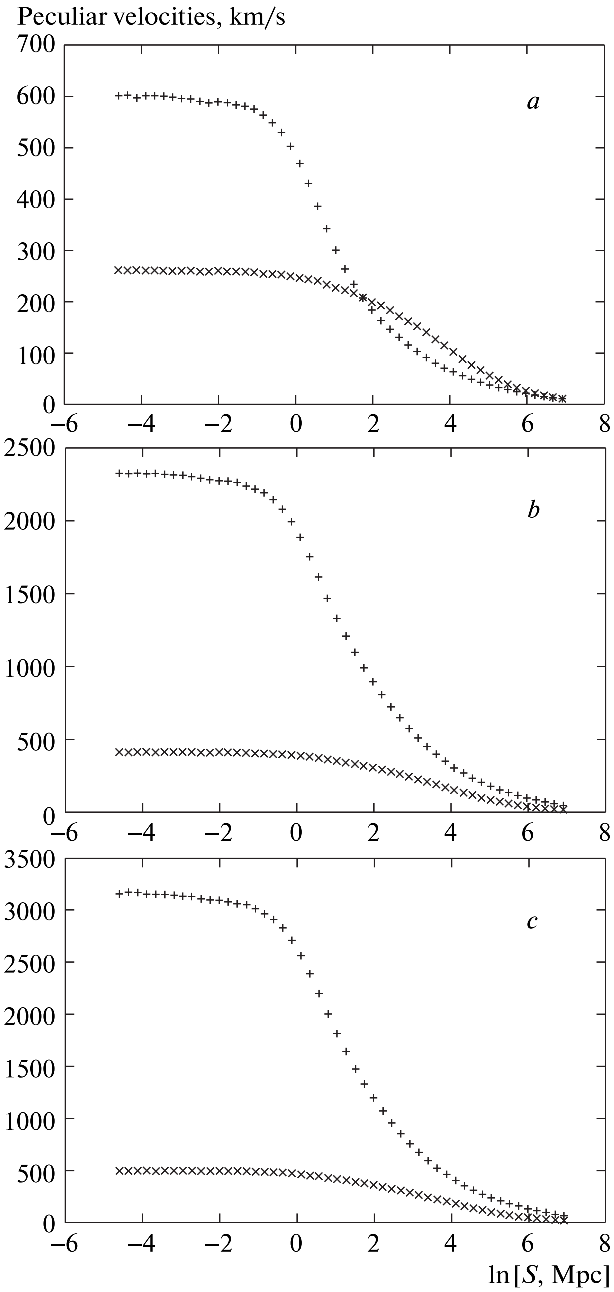

Fig. 3. Peculiar velocities for three redshifts ($z = 1$ (a), 0.25 (b), and 0 (c)) as functions of the scale S. EC — $+$, ΛCDM — $\times$

ΛCDM cosmology at the galaxy and galaxy cluster scales $\mathcal{O}(10^{-1})$ Mpc – $\mathcal{O}(10^2)$ Mpc.

The conclusions are not sensitive to the reasonable choices of the parameters of the clustering model. The integrated Sachs–Wolfe effect plays an important role at low redshifts in the evolution, if the mass density differs from unity [13]:

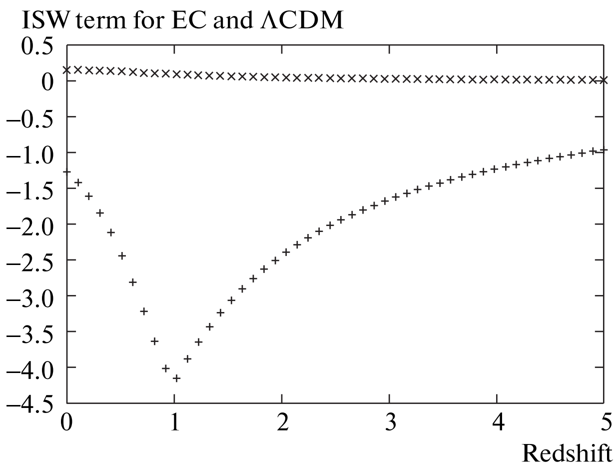

Fig. 4. Integrated Sachs–Wolfe terms χ^{ISW} for EC ($+$) and ΛCDM ($\times$) cosmologies

$$
\begin{gathered}
a_{lm}^{ISW} = 12\pi i^l \int d^3k Y_l^{m*}(\hat{k})\delta_{\vec{k}} \left(\frac{H_0}{k}\right)^2 \times \\
\times \int da j_l(kr)\chi^{ISW}, \\
\chi^{ISW}(a) = -\Omega_m \frac{d}{da}\left(\frac{\delta(a)}{a}\right), \\
r = \int_a^1 da\, a^{-2} H^{-1}(a), \quad \delta(a=1) = 1.
\end{gathered}
\tag{10}
$$

The ISW is positive (negative) for the ΛCDM (EC) cosmology (see Fig. 4). The structure of the EC ISW curve around $z = 1$ is just an artefact of our simple model for torsion with a nonanalytic behavior at $z = 1$.

The compendium of all our results can be summarized as follows: (1) the ΛCDM model cannot simultaneously fit the large and the small scale parts of the Planck TT spectrum, while the EC can rectify this deficiency owing to the presence of the new rotational degrees of freedom (torsion) that partially cancels the large mass density ($\Omega_m = 2$) when clustering matters, i. e., rotation (the centripetal force) acts opposite to the attractive force of gravity, (2) the presence of the ISW effect is observed in Planck data [19], but with the unknown sign; the very small low multipoles of the Planck TT spectrum imply the negative contribution of the ISW [20], which agrees with the EC model, (3) the peculiar velocities are larger at the galaxy and galaxy cluster scales for the EC than ΛCDM cosmologies at low redshifts. These conclusions are robust and are qualitatively valid for a reasonable variation of the clustering model parameters k_G and σ_G. The two different analyses of the Planck peculiar velocities of galaxy clusters [21] are still not conclusive as to whether the data are consistent with the ΛCDM model.

Our final remark is that the first Planck results favor a description of the Universe with anisotropic models. The ΛCDM and the inflationary paradigm cannot fulfil severe phenomenological requirements. We show that the EC cosmology with the new rotational degrees of freedom can resolve almost all of the ΛCDM model deficiencies. However, the N-body numerical simulations, including the angular momenta of the CDM halos and their feedback onto the background cosmic geometry, have to be applied within the EC gravity.

REFERENCES

1. C. L. Bennett et al., Astrophys. J. Suppl. Ser. **148**, 1 (2003).
2. Planck Collab., arXiv:1303.5075.
3. Planck Collab., arXiv:1303.5083.
4. P. Birch, Nature **298**, 451 (1982).
5. M. J. Longo, Phys. Lett. B **699**, 224 (2011).
6. A. Kashlinsky, F. Atrio-Barandela, D. Kocevski, and H. Ebeling, Astrophys. J. Lett. **686**, L49 (2008).
7. D. Hutsemékers, Astron. and Astrophys. **332**, 410 (1998).
8. A. Trautman, Nature **242**, 7 (1973).
9. D. Palle, Nuovo Cim. B **111**, 671 (1996).
10. D. Palle, Nuovo Cim. B **122**, 67 (2007).
11. D. Palle, Nuovo Cim. B **114**, 853 (1999).
12. D. Palle, Entropy **14**, 958 (2012).
13. D. Palle, Eur. Phys. J. C **69**, 581 (2010).
14. D. Palle, Nuovo Cim. A **109**, 1535 (1996).
15. D. Palle, Nuovo Cim. B **115**, 445 (2000); ibid **118**, 747 (2003).
16. D. Palle, Hadronic J. **24**, 87 (2001); ibid **24**, 469 (2001); D. Palle, Acta Phys. Pol. B **43**, 1723 (2012); ibid **43**, 2055 (2012); D. Palle, arXiv:1210.4404.
17. P. J. E. Peebles, *The Large-Scale Structure of the Universe*, Princeton University Press, New Jersey (1980); P. J. E. Peebles, Astrophys. J. **277**, 470 (1984).
18. T. Hahn, Comp. Phys. Commun. **168**, 78 (2005).
19. Planck Collab., arXiv:1303.5079.
20. H. Kodama and M. Sasaki, Prog. Theor. Phys. Suppl. **78**, 1 (1984).
21. Planck Collab., arXiv:1303.5090; F. Atrio-Barandela, arXiv:1303.6614 (to appear in Astron. and Astrophys.).